

# In Situ Observation of Crack Behavior in Compressively Loaded Plasma-Sprayed 7-wt%-Yttria-Stabilized Zirconia

Jonathan P. Levin, Graeme R. Dickinson,\* and Rodney W. Trice\*

School of Materials Engineering, Purdue University, West Lafayette, Indiana 47906

**A plasma-sprayed 7-wt%-yttria-stabilized zirconia stand-alone tube was incrementally loaded in uniaxial compression inside a scanning electron microscope. Micrographs taken at each increment showed cracks perpendicular to the applied load to have partially closed and cracks parallel to the applied load to have opened. New cracks were observed to nucleate and then propagate in a direction parallel to the applied load.**

## I. Introduction

PLASMA-SPRAYED yttria-stabilized zirconia (YSZ) is commonly used as a thermal barrier coating (TBC) in gas-turbine applications. These low-thermal-conductivity coatings afford higher, more efficient engine operating temperatures. The plasma-spraying technique results in a microstructure containing flattened lamellae stacked on each other with a significant amount of porosity and microcracks in and between the lamellae. Of particular interest in this study is how the network of microcracks and their orientation affects the mechanical behavior of the coating. For example, there is evidence that the compressive modulus of some plasma-sprayed materials increases under increasing applied loads. This has been observed in plasma-sprayed 8 wt% yttria-zirconia<sup>1</sup> and alumina.<sup>2</sup> It has been speculated that the increase in modulus is a result of microcrack closure caused by loading of the plasma-sprayed coating. Another characteristic feature of plasma-sprayed materials is loading/unloading hysteresis; this behavior has been attributed to the formation of microcracks during loading<sup>2,3</sup> that do not cause catastrophic failure.

For this investigation, stand-alone 7 wt% yttria-zirconia cylindrical tubes were prepared and tested incrementally under axial compression using a load frame in an environmental scanning electron microscope (ESEM). Micrographs of the sample were taken after each loading increment and compared with the stress-strain response of the coating. The response of cracks perpendicular and parallel to the applied load was observed.

## II. Material and Procedures

Stand-alone samples of YSZ were created with a cylindrical geometry using a control system (Model A-3000, Plasma Technik, Siegen, Germany) equipped with a gun (Model F4) mounted on a seven-axis robot (Model IRB 2000, ASEA Brown and Boveri, Billingstad, Norway). The gun was operated at 35 kW. These samples were created by first plasma spraying aluminum powder (54NS-1, Sulzer Metco, Westbury, NY) onto a 30 cm long alumina rod with a diameter of 1.27 cm, followed by plasma spraying a 280

μm YSZ (~15 μm powder, Amperit 825.0, H.C. Starck, Newton, MA) layer. The YSZ was fed into the plasma using a 30°-angled small-particle plasma-spray injector<sup>4</sup> and a conventional disk feeder. The spray distance, as measured from the injector to the substrate, was 6 cm. The argon primary-gas flow was 32 standard liters per minute (slm) and the hydrogen secondary-gas flow was 8 slm. The argon carrier gas flow was 5 slm.

Multiple tubes of a height of 20 mm were cut from the 30 cm long coated rod. The tubes were then immersed in a weak solution of HCl, which dissolved the aluminum, releasing the stand-alone YSZ tubes. As determined using  $K\alpha$  X-ray diffraction, the YSZ coating consisted of an yttrium-rich, nonequilibrium tetragonal-zirconia phase. The coatings exhibited a bulk density of ~5.2 g/cm<sup>3</sup>, with a total porosity of ~15%.

Two strain gauges<sup>1</sup> were attached to the outer surface of the YSZ sample investigated, ~180° from one another, using a thin layer of epoxy. The gauges were oriented so that axial strain was measured. The difference in the axial strain between the two strain gauges was used to align the sample within the load frame. Alignment was adjusted using thin metal shims placed behind the stainless-steel loading brackets of the load frame. The sample was located between these blocks during testing.

The sample was tested in compression in an load frame (Model 8500 Plus, Instron Corp., Danvers, MA) that was physically located in an ESEM (Model 2020, ElectroScan GmbH, Berlin, Germany). The ESEM was operated at a working distance of 27.2 mm, an accelerating voltage of 25 keV, and chamber pressures of 1.5 and 3.5 torr (200 and 470 Pa). The sample was compressed incrementally until fracture using stress increments of ~13 and 8 MPa. The smaller stress increment was used after loading the sample to 104 MPa. Micrographs at several magnifications were taken after each stress increment. Strain values at each increment were taken manually from a strain indicator (Model P-350A, Vishay Instruments, Malvern, PA). The scale bars for the micrographs were calibrated by viewing a grid of known size using the same detector, working distance, and magnification as were used during the experiment.

## III. Results

The stress-strain response from the incrementally loaded YSZ tube is shown in Fig. 1. The strain data represent an average of the two strain gauges. The sample reached a compressive stress of  $137 \pm 2$  MPa, but critical failure occurred before strain data could be taken at that stress.

Although multiple modulus values can be calculated from the stress-strain response in Fig. 1, the data are treated as having two distinct slopes. The first region, which occurs at applied stresses  $< 46 \pm 1$  MPa, has a modulus of ~30 GPa; the second region, which occurs at applied stresses  $> 46 \pm 1$  MPa, has a modulus of ~60 GPa. The two distinct slopes are indicative of the fact that the modulus has increased in the sample as a result of the applied load. Although the bulk modulus of dense zirconia is ~200 GPa,<sup>5</sup> current values are within the same order of magnitude as other reported values for the compressive modulus of plasma-sprayed YSZ.<sup>1,6</sup>

The region investigated in the ESEM during loading was the outer surface of the YSZ tube; this region was chosen because it

M. Thouless—contributing editor

Manuscript No. 10480. Received August 21, 2003; approved December 12, 2003. Supported by the National Science Foundation through Grant Nos. DMR-0134286 and DMR-0243830.

\*Member, American Ceramic Society.

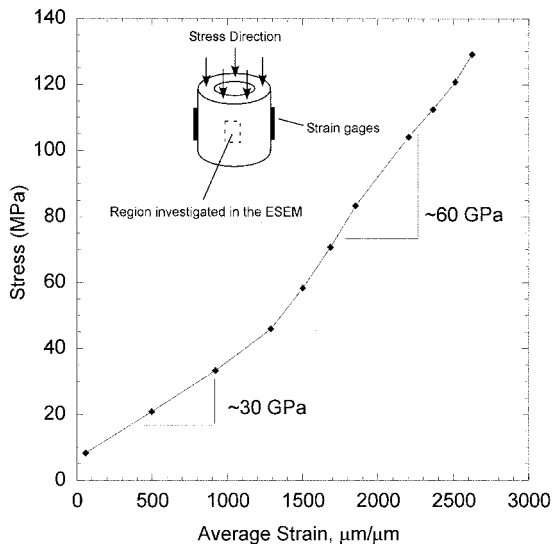


**Fig. 1.** Stress-strain curve of YSZ tube that shows a distinct change in the slope as stress increases. Two modulus regions in the stress-strain curve are highlighted.

contained cracks of various widths oriented parallel, perpendicular, and off-axis (or angled) with respect to the applied load. Figure 2 shows the specific regions of longer cracks investigated in this study under no load; these included two cracks oriented vertically and three cracks oriented horizontally with respect to the applied stress. These particular cracks were likely the result of thermal stresses that occurred during cooling of the plasma-sprayed coating. Figures 3 and 4 are micrographs of the YSZ surface taken at loading increments of  $71 \pm 1$  MPa and  $129 \pm 2$  MPa, respectively. Comparison of Figs. 2, 3, and 4 shows that cracks oriented parallel to the loading direction have opened, while cracks oriented perpendicular to the loading direction have partially closed as a result of the applied stress.

The number of crack openings or closures was quantified by measuring the distance across the cracks as a function of applied stress. The results are presented in Fig. 5. For example, horizontal crack 3, which initially was  $0.8 \mu\text{m}$  in width, closed to  $0.4 \mu\text{m}$  under an applied stress of  $130 \pm 2$  MPa. Similar trends were observed in the other two horizontal cracks investigated. The opposite trend was observed in cracks oriented vertically with respect to the load. Vertical crack 1 opened from  $1$  to  $1.5 \mu\text{m}$  under an applied stress of  $130 \pm 2$  MPa.

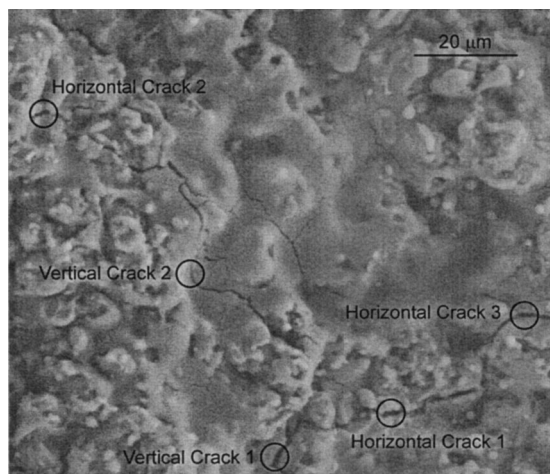


**Fig. 2.** SEM micrograph of the investigated area on the outer surface of the YSZ tube before loading; the locations where crack width were measured before and during loading are indicated.

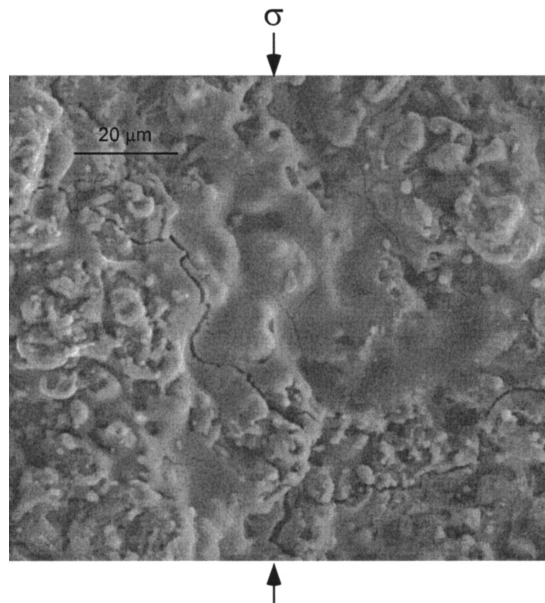


**Fig. 3.** SEM micrograph of the sample under a compressive stress of  $71 \pm 1$  MPa. Comparison of this micrograph with Fig. 2 reveals that cracks oriented perpendicular to applied load (i.e., horizontal cracks) have slightly closed and cracks oriented parallel to applied load (i.e., vertical cracks) have further opened.

#### IV. Discussion

As stated in the Introduction, previous mechanical experiments on plasma-sprayed ceramic coatings have shown that the modulus of the material increases as load increases. This is observed in the current data set, as shown in Fig. 1. It has been hypothesized that the increase in modulus is caused by cracks oriented perpendicular to the applied load becoming partially or completely closed.<sup>2</sup> Figures 3 and 4 seem to confirm that this explanation is plausible in that cracks oriented perpendicular to the loading application exhibit a decrease in width. The observed increase in modulus with partial crack closure can be

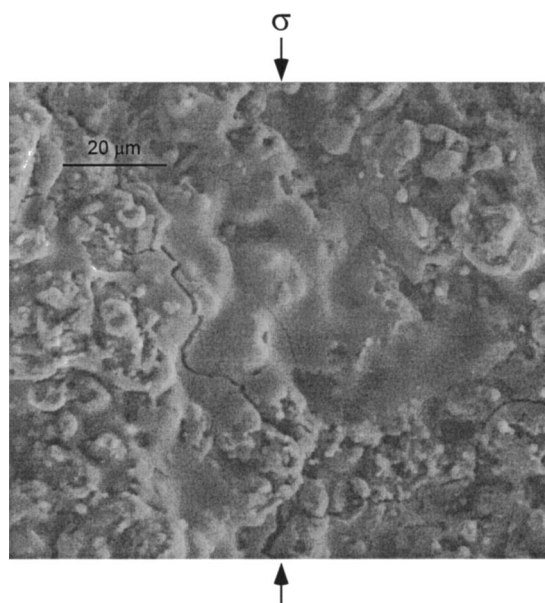


**Fig. 4.** SEM micrograph of the sample under a compressive stress of  $129 \pm 2$  MPa. Comparison of this micrograph with Figs. 2 and 3 reveals that cracks oriented perpendicular to applied load have further closed and cracks oriented parallel to applied load have continued to open.

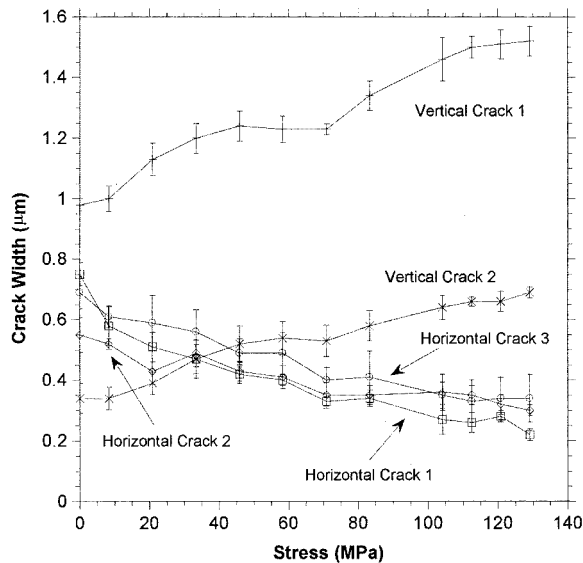


**Fig. 5.** Plot of crack width versus stress for five crack locations measured in the SEM micrographs taken at various loadings. Locations 1–3 show cracks oriented perpendicular to the applied load to have closed; locations 4 and 5 show cracks oriented parallel to the applied load to have opened. Error bars were calculated based on repeated width measurements of the same area.

explained by the fact that, as cracks oriented perpendicular to the stress close, a larger area fraction of the load is carried by the YSZ.

The reason that cracks oriented parallel with respect to the imposed stress open can be deduced by considering the full length of the observed crack. For example, in Fig. 2, the area labeled vertical crack 1 is part of a much larger crack that includes horizontal cracks 1 and 2. Although a section of this crack is oriented parallel with respect to the imposed stress (i.e., vertical crack 1), portions of that same crack are oriented such that they are off the main loading axis. Ashby and Hallam<sup>7</sup> studied the response of angled cracks loaded in compression in a 1986 paper. They observed that cracks oriented between 30° and 60° with respect to the loading axis had a significant shear component between the crack faces. As the crack faces slide relative to one another under the shear stress, they tend to nucleate and propagate cracks parallel with respect to the loading axis. In the crack studied presently, it appears that sliding of crack faces in angled cracks tends to further open the vertically oriented crack.

One region of the sample investigated that demonstrates crack nucleation and propagation is shown in Fig. 6. These micrographs show that, at  $33 \pm 1$  MPa, no crack has yet initiated, but, in the micrograph taken of the sample at a stress of  $58 \pm 1$  MPa, a small crack has initiated from the edge of an angled crack. This crack propagates in a direction roughly parallel to the applied stress, consistent with the results of Ashby and Hallam<sup>7</sup> described previously. Additionally, Ashby and Hallam showed that microcracking occurs at about half of the failure stress of a brittle solid.<sup>7</sup> The second micrograph taken at a stress of  $58 \pm 1$  MPa concurs with this observation, and it shows the initial stages of microcrack formation at approximately half of the failure stress of the stand-alone tube ( $137 \pm 2$  MPa).

The micrographs in Fig. 6, which were taken when the tube was loaded to stresses of  $83 \pm 1$  and  $129 \pm 2$  MPa, show that, as the stress increased, the length and the width of the crack increased. This is important, because it shows that new microcracks can exhibit stable propagation before catastrophic failure, which is consistent with prior observations.<sup>7</sup>

## V. Summary and Conclusions

A thin, stand-alone yttria-stabilized zirconia plasma-sprayed tube was subjected to an incremental compressive stress inside a

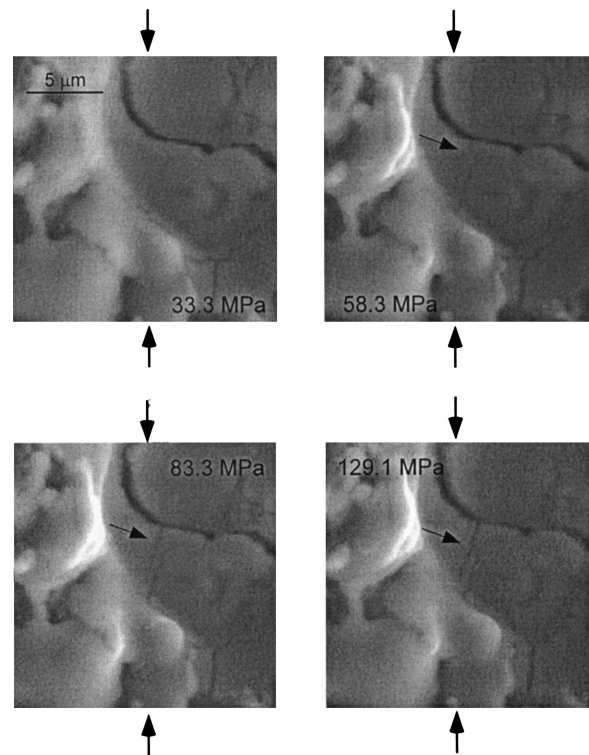


**Fig. 6.** SEM micrographs of the same region of the sample at multiple stress levels. It was observed that a crack nucleated at an applied stress of  $58 \pm 1$  MPa. It originated from an angled crack and propagated in a stable manner as stress was increased to  $83 \pm 1$  and  $129 \pm 2$  MPa.

scanning electron microscope until critical failure. The behavior of cracks in the sample was observed at various stress intervals, and strain data were taken.

The stress–strain curve consisted of at least two distinct slopes that exhibited increased modulus with increased stress. The micrographs taken during incremental loading showed that cracks oriented roughly perpendicular to the applied load partially closed and that cracks oriented roughly parallel to the applied load opened further. The closure of cracks oriented perpendicular to the applied stress caused increased planar density of the sample, which, in turn, caused the increased modulus shown in the stress–strain curve. Also, a small microcrack was observed to form at roughly half of the failure stress of the sample from an existing angled crack. The new crack propagated roughly in the direction parallel to the applied stress. This agreed with previous research done on the failure of brittle solids, where cracks initiated from the ends of angled cracks and propagated in the direction of the applied stress.<sup>7</sup>

## Acknowledgments

The authors wish to thank Jan Eberle for his technical support with the ESEM.

## References

- <sup>1</sup>K. F. Wesling and D. F. Socie, "Fatigue of Thick Thermal Barrier Coatings," *J. Am. Ceram. Soc.*, **77** [7] 1863–68 (1994).
- <sup>2</sup>R. W. Trice, D. W. Prine, and K. T. Faber, "Deformation Mechanisms in Compression-Loaded Stand-Alone Plasma-Sprayed Alumina Coatings," *J. Am. Ceram. Soc.*, **83** [12] 3057–64 (2000).
- <sup>3</sup>E. F. Rejda, D. F. Socie, and B. Beardsley, "Fatigue Behavior of a Plasma-Sprayed 8%  $Y_2O_3$ - $ZrO_2$  Thermal Barrier Coating," *Fatigue Fract. Eng. Mater. Struct.*, **20** [7] 1043–50 (1997).
- <sup>4</sup>T. F. Bernecki and D. R. Marron, "Small Particle Plasma Spray Apparatus, Method, and Coated Article," U.S. Pat. No. 5 744 777, Apr. 28, 1998.
- <sup>5</sup>R. Stevens, "Introduction to Zirconia," Publication No. 13, p. 31, Magnesium Elektron, Flemington, NJ, 1986.
- <sup>6</sup>T. A. Cruse, B. P. Johnsen, and A. Nagy, "Mechanical Properties Testing and Results for Thermal Barrier Coatings," *J. Therm. Spray Technol.*, **6** [1] 57–66 (1997).
- <sup>7</sup>M. F. Ashby and S. D. Hallam, "The Failure of Brittle Solids Containing Small Cracks Under Compressive Stress States," *Acta Metall.*, **34** [3] 497–510 (1986). □